

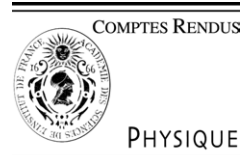


ELSEVIER

Available online at [www.sciencedirect.com](http://www.sciencedirect.com)

SCIENCE @ DIRECT®

C. R. Physique 6 (2005) 337–344



<http://france.elsevier.com/direct/COMREN/>

The Near Earth Objects: possible impactors of the Earth/Les astéroïdes géocroiseurs impacteurs  
potentiels de la Terre

# Close encounters and collisions of Near-Earth asteroids with the Earth

Giovanni B. Valsecchi

*INAF-IASF, via Fosso del Cavaliere 100, 00133 Rome, Italy*

Available online 17 February 2005

Presented by Pierre Encrenaz

---

## Abstract

This article describes some recent advances in the analytical theory of close encounters between small bodies and the Earth. This theory is based on the work of Öpik, and allows us to understand the main geometrical features of close encounters leading to resonant returns, a very important phenomenon to be taken into account in the analysis of the dynamical evolution of Earth crossing asteroids. *To cite this article: G.B. Valsecchi, C. R. Physique 6 (2005).*

© 2005 Académie des sciences. Published by Elsevier SAS. All rights reserved.

## Résumé

**Rencontres proches et collisions des astéroïdes géocroiseurs avec la Terre.** Ce papier décrit les développements récents de la théorie analytique des rencontres proches entre petits corps et la Terre. Cette théorie est basée sur celle de Öpik et permet de comprendre la géométrie des rencontres proches amenant à des retours résonnants, ce qui est un phénomène très important, qui doit être tenu en compte dans l'analyse de l'évolution dynamique des astéroïdes géocroiseurs. *Pour citer cet article : G.B. Valsecchi, C. R. Physique 6 (2005).*

© 2005 Académie des sciences. Published by Elsevier SAS. All rights reserved.

*Keywords:* Asteroids; Dynamics; Close encounters

*Mots-clés:* Astéroïdes; Dynamique; Rencontres proches

---

## 1. Introduction

The role of close encounters with the planets in the orbital evolution of small solar system bodies has been recognized already at the end of the XVIIIth century by Lexell [1], in his study of the comet that is now known as comet D/Lexell.

Lexell was the first to understand that the lack of observations of that comet prior to 1770 was due to an orbital change caused by a close encounter with Jupiter in 1767, and predicted that a similar encounter would take place in 1779, and would put again the comet into an unobservable orbit. The separation in time between the two encounters corresponds almost exactly to one revolution of Jupiter and to two revolutions of the comet on the orbit it had between 1767 and 1779; thus, the second encounter of comet D/Lexell with Jupiter is the consequence of the fact that the first had put the comet into a nearly-resonant orbit, of period one half of that of the orbit of Jupiter. Using current terminology, the second encounter of D/Lexell with Jupiter is a *resonant return* [2].

---

*E-mail address:* [giovanni@rm.iasf.cnr.it](mailto:giovanni@rm.iasf.cnr.it) (G.B. Valsecchi).

Le Verrier, working a few decades after Lexell, examined again the motion of the same comet [3–5]. He was interested in evaluating how well the available observations constrained the orbital elements of the comet, and found that it was not possible to determine a unique orbit, since the constraints given by the observations were insufficient. He then expressed the six orbital elements of D/Lexell as functions of a single unknown parameter, that he called  $\mu$ , using the observations to find the admissible range of variation of  $\mu$ .

Le Verrier computed the effects of the 1767 and 1779 encounters with Jupiter on the orbit for various values of  $\mu$ , so as to obtain a global view of all the possible outcomes – much like the systematic computations of virtual asteroids carried out nowadays. He established, among other things, that the comet could approach Jupiter extremely closely in 1779, as close as less than three and a half radii of the planet from its centre; nevertheless, the comet could not become a satellite of Jupiter, not even temporarily, for any allowed value of  $\mu$ . The range of post-1779 orbits included even the possibility for the comet to leave the solar system on a hyperbolic orbit. The reason for this wide range of possible outcomes was the extreme sensitivity of the subsequent evolution to the precise value adopted for  $\mu$ . This sensitivity is a crucial part of the modern concept of chaos, and in fact Le Verrier's computations probably represent the first instance of this concept in scientific literature.

Examining the set of elements adopted by Le Verrier, it is easy to realize that the region allowed for his orbital solution was very small in all elements, except semimajor axis and eccentricity, and that the variation allowed for these two elements is such that the perihelion distance is constant. In fact, a comparison of Le Verrier's elements with those adopted much later by Carusi et al. [6] to simulate a meteor stream, ejected at the perihelion passage of 1770 by the comet, shows that in fact the range allowed by Le Verrier for the parameter  $\mu$  was mostly determined by the uncertainty in the magnitude of the velocity vector of the comet, amounting to  $\pm 10$  m/s at perihelion.

In the last few years the interest in the study of close planetary encounters has been revived by the analysis of the motions of Near-Earth Asteroids (NEAs), that are being discovered at a much higher rate since 1998. This analysis is routinely carried out by the specialized software robots running at the Universities of Pisa and Valladolid, and at the Jet Propulsion Laboratory [7–9].

Some geometrical understanding of the close encounters of NEAs with the Earth has been obtained by means of a suitable extension of the well-known analytical theory of close encounters due to Öpik [10] (see also [11]). Hereafter, based on [12], we discuss the main algorithms that allow us to understand the geometry of resonant returns.

## 2. Extended Öpik's theory of close encounters

The model on which Öpik's theory of close encounters is based is a simplified version of the restricted, circular, 3-dimensional 3-body problem. In fact, in the theory it is assumed that, far from the planet, the small body moves on an unperturbed heliocentric keplerian orbit.

The encounter with the planet is then modelled as an instantaneous transition from the incoming asymptote of the planetocentric hyperbola to the outgoing one, taking place when the small body crosses the plane orthogonal to the small body unperturbed velocity vector,  $\mathbf{U}$ , containing the centre of the planet, called  $b$ -plane.

In [12] the basic theory has been extended by adding suitable equations to take into account the nodal distance and the time of passage of the small body at the node. However, this model does not take into account the secular variation of the nodal distance, that has to be given as an additional input.

The equations of motion near the planet are defined in the reference frame  $(X, Y, Z)$ , centred on the planet; the  $Y$ -axis is in the direction of motion of the planet, and the Sun is on the negative  $X$ -axis. At time  $t_0$  the small body is at the node, and its coordinates are  $(X_0, Y_0, 0)$ .

The magnitude of the velocity vector  $\mathbf{U}$  is

$$U = \sqrt{3 - \frac{1}{a} - 2\sqrt{a(1 - e^2)} \cos i},$$

and its direction is defined by two angles,  $\theta$  and  $\phi$ , such that

$$\begin{bmatrix} U_x \\ U_y \\ U_z \end{bmatrix} = \begin{bmatrix} U \sin \theta \sin \phi \\ U \cos \theta \\ U \sin \theta \cos \phi \end{bmatrix}.$$

The angles  $\theta$  and  $\phi$  can be computed from the orbital elements:

$$\theta = \arccos \frac{\sqrt{a(1 - e^2)} \cos i - 1}{\sqrt{3 - 1/a - 2\sqrt{a(1 - e^2)} \cos i}},$$

$$\phi = \arctan \frac{\pm \sqrt{2 - 1/a - a(1 - e^2)}}{\pm \sqrt{a(1 - e^2)} \sin i};$$

the numerator in the expression of  $\phi$  is positive if the encounter takes place in the post-perihelion branch of the orbit of the NEA, and negative otherwise, while the denominator is positive if the encounter takes place at the ascending node of the orbit, and negative otherwise.

### 2.1. The pre-encounter state vector

The pre-encounter state vector  $\mathbf{V}$ , that completely describes the dynamical state of the small body, has components  $(U, \theta, \phi, \xi, \zeta, t_0)$ , where  $(\xi, \zeta)$  are the coordinates on the  $b$ -plane. Neglecting terms of the second order in the miss distance at the node, the components of the vector  $\mathbf{b}$  extending from the planet to the intersection of the incoming asymptote with the  $b$ -plane, are

$$\begin{bmatrix} \xi \\ \zeta \end{bmatrix} = \begin{bmatrix} \cos \phi \left[ \frac{a(1-e^2)}{1 \pm e \cos \omega} - 1 \right] \\ \xi \cos \theta \tan \phi - \sin \theta \left( 1 + \frac{\xi}{\cos \phi} \right) \tan(\Omega - \lambda_{\oplus} - \pi/2 \pm \pi/2) \end{bmatrix}, \quad (1)$$

where the upper sign applies at encounters at the ascending node, and  $\lambda_{\oplus}$  is the longitude of the Earth at time  $t_0$ . The orientations of these two axes are such that  $\zeta$  is anti-parallel to the projection of the  $Y$ -axis on the  $b$ -plane, and  $\xi$  is perpendicular to both  $\mathbf{U}$  and the  $Y$ -axis. It can be shown that the local Minimum Orbital Intersection Distance (MOID, i.e. the minimum distance between the orbit of the small body and that of the Earth) is given by  $\xi$ , and that it is tied to the distance from the node  $X_0$  by the simple expression [12]

$$\xi = X_0 \cos \phi.$$

### 2.2. The post-encounter state vector

The close encounter can be seen as an operator  $\mathbf{E}$  that maps the pre-encounter state vector

$$\mathbf{V} \equiv (U, \theta, \phi, \xi, \zeta, t_0)$$

into the post-encounter one

$$\mathbf{V}' \equiv (U', \theta', \phi', \xi', \zeta', t_0')$$

so that

$$\mathbf{V}' = \mathbf{E}\mathbf{V}.$$

The components of  $\mathbf{V}'$ , as functions of those of  $\mathbf{V}$ , are

$$\begin{aligned} U' &= U, \\ \theta' &= \arccos \left[ \frac{(b^2 - c^2) \cos \theta + 2c\zeta \sin \theta}{b^2 + c^2} \right] \\ &= \arcsin \left[ \frac{\sqrt{[(b^2 - c^2) \sin \theta - 2c\zeta \cos \theta]^2 + 4c^2\xi^2}}{b^2 + c^2} \right], \\ \phi' &= \arccos \left[ \frac{[(b^2 - c^2) \sin \theta - 2c\zeta \cos \theta] \cos \phi + 2c\xi \sin \phi}{\sqrt{[(b^2 - c^2) \sin \theta - 2c\zeta \cos \theta]^2 + 4c^2\xi^2}} \right] \\ &= \arcsin \left[ \frac{[(b^2 - c^2) \sin \theta - 2c\zeta \cos \theta] \sin \phi - 2c\xi \cos \phi}{\sqrt{[(b^2 - c^2) \sin \theta - 2c\zeta \cos \theta]^2 + 4c^2\xi^2}} \right], \\ \xi' &= \frac{(b^2 + c^2)\xi \sin \theta}{\sqrt{[(b^2 - c^2) \sin \theta - 2c\zeta \cos \theta]^2 + 4c^2\xi^2}}, \\ \zeta' &= \frac{(b^2 - c^2)\zeta \sin \theta - 2b^2c \cos \theta}{\sqrt{[(b^2 - c^2) \sin \theta - 2c\zeta \cos \theta]^2 + 4c^2\xi^2}}, \\ t_0' &= \frac{2c[\xi \sin \phi (2\zeta \cos \theta - \xi \tan \phi) - \cos \phi (\xi^2 \sin^2 \theta + \zeta^2)]}{U \sin \theta [(b^2 - c^2) \sin \theta - 2c\zeta \cos \theta] \cos \phi + 2c\xi \sin \phi} + t_0, \end{aligned}$$

with  $b = |\mathbf{b}|$  and  $c = m/U^2$ , where  $m$  is the mass of the Earth.

### 2.3. The propagation to the next encounter

After the first close approach, the motion until the next encounter is treated as a keplerian propagation, i.e. as an operator  $\mathbf{P}$  that maps the post-encounter state vector  $\mathbf{V}'$  in the pre-next-encounter one

$$\mathbf{V}'' \equiv (U'', \theta'', \phi'', \xi'', \zeta'', t_0'')$$

so that

$$\mathbf{V}'' = \mathbf{P}\mathbf{V}'.$$

The transformation is given by:

$$\begin{aligned} U'' &= U', \\ \theta'' &= \theta', \\ \phi'' &= \phi', \\ \xi'' &= \xi', \\ \zeta'' &= \zeta' - [\text{mod}(h \cdot 2\pi a'^{3/2} + \pi, 2\pi) - \pi] \sin \theta', \\ t_0'' &= t_0' + h \cdot 2\pi a'^{3/2}, \end{aligned}$$

where  $h$  is the number of revolutions of the NEA in its orbit and, to a good level of approximation, the post encounter semimajor axis is given by

$$a' = \frac{b^2 + c^2}{(b^2 + c^2)(1 - U^2) - 2U[(b^2 - c^2) \cos \theta + 2c\zeta \sin \theta]}.$$

#### 2.3.1. The MOID and its variation with time

A problem for this type of modelling, which is based on a purely keplerian propagation between encounters, is that there are large short-period variations superimposed on a secular trend. In order to get the basic geometric features of the problem, we can model the variation of the MOID using a simple linear secular trend:

$$\xi'' = \xi' + \dot{\xi} \cdot h \cdot 2\pi a'^{3/2},$$

where the time derivative of  $\xi$  can be computed, e.g., using a value taken from a numerical integration or from a secular theory of crossing orbits [13].

## 3. Close encounters and keyholes

In order to understand the structure of subsequent encounters between a small body and the Earth the concept of *keyhole* was introduced by Chodas [14]. A *keyhole* is a small region of the  $b$ -plane of a specific close encounter of an asteroid with the Earth such that, if the asteroid passes through it, it will hit the planet or anyway have a very close encounter with it at a subsequent return.

We can think of the keyholes also as the regions on the  $b$ -plane such that, if the small body passes through one of them, it is put in an orbit of given period/semimajor axis. Putting things in this way, an interesting new result is that the locus of the  $b$ -plane points leading to a final orbit of given semimajor axis is a circle, whose radius and coordinates of the centre are functions only of  $U$ ,  $\theta$  and  $\theta'$ .

### 3.1. The resonant circles

A given resonance corresponds to a certain value of  $a'$ , i.e. of  $\theta'$ , say  $a'_0$  and  $\theta'_0$ . Assume that the ratio of the periods of the small body and of the Earth is  $k/h$ . Then, following a first encounter, after  $h$  heliocentric revolutions of the small body and  $k$  revolutions of the Earth, both the Earth and the small body will be back to the same position of the previous encounter, performing a resonant return.

The locus of the points leading to a resonant return can be calculated starting from the values of  $a'_0$  and  $\theta'_0$ , given by

$$a'_0 = (k/h)^{2/3},$$

$$\cos \theta'_0 = \frac{1 - U^2 - 1/a'_0}{2U}$$

but also, from the geometry of the deflection,

$$\cos \theta'_0 = \frac{(b^2 - c^2) \cos \theta + 2c\zeta \sin \theta}{b^2 + c^2}.$$

Since  $b^2 = \xi^2 + \zeta^2$ , we obtain [15]

$$\xi^2 + \zeta^2 - 2D\zeta + D^2 - R^2 = 0,$$

i.e., the equation of a circle of radius  $|R|$  centred in  $(0, D)$ , with

$$R = \frac{c \sin \theta'_0}{\cos \theta'_0 - \cos \theta},$$

$$D = \frac{c \sin \theta}{\cos \theta'_0 - \cos \theta}.$$

### 3.2. The location of the keyholes

The region of incertitude of a NEA is the region in orbital elements' space in which the NEA orbit is confined by stipulating that the observational errors are within given bounds. It is in general modelled, under suitable assumptions [16], as an ellipsoid in elements' space. For epochs sufficiently separated in time from the observations, the ellipsoid becomes more and more elongated, essentially along the axis corresponding to the mean anomaly. In fact, while small differences in the values of  $e, i, \omega$  and  $\Omega$ , allowed by the observational record, will not change appreciably between the epoch of observations and that of the first close planetary encounter, a small difference in  $a$  would lead to a secular spreading of the mean anomaly.

When there is a close encounter with the Earth, the intersection of this region with the  $b$ -plane is nearly parallel to the  $\zeta$ -axis, with the  $\xi$  coordinate equal to the MOID. This can be understood by looking at the definitions of  $\xi$  and  $\zeta$  (Eq. (1)). In fact, the spread in mean anomaly translates into a corresponding spread in  $t_0$ ; thus, the longitude of the Earth  $\lambda_{\oplus}$ , appearing in (1), varies for different locations within the confidence region. Since  $\xi$  does not depend on  $\lambda_{\oplus}$ , only  $\zeta$  is affected.

As a consequence, the possible locations of keyholes are the intersections with the appropriate resonant  $b$ -plane circle with a straight line parallel to the  $\zeta$ -axis, at  $\xi$  equal to the MOID.

Fig. 1 shows the arrangement of the  $b$ -plane circles corresponding to resonant returns to close encounter in 2040, 2044, 2046 for the August 2027 encounter with the Earth of asteroid 1999 AN<sub>10</sub> [2]; these correspond, respectively, to the mean motion resonances 7/13, 10/17, and 11/19. In the plot a straight line at  $\xi = 6$  terrestrial radii is also drawn, that represents a string of

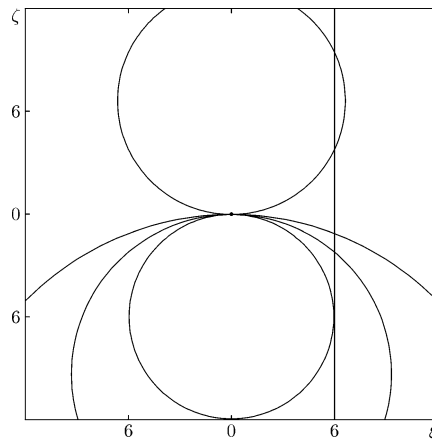


Fig. 1. Circles corresponding to various mean motion resonances on the  $b$ -plane of the August 2027 encounter with the Earth of asteroid 1999AN<sub>10</sub>. Uppermost circle: 7/13 resonance, leading to an encounter in 2040; then, with the centres along the  $\zeta$ -axis, from top to bottom: 3/5, 10/17 and 11/19 resonances, leading to encounters in 2032, 2044, 2046, respectively. Distances are in Earth radii; the vertical line at  $\xi = 6$  represents fictitious asteroids all with the same orbital parameters as 1999 AN<sub>10</sub> and spaced in the time of encounter with the Earth.

fictitious asteroids having the same orbit and MOID (and thus the same  $\xi$ ), and spaced in the timing of encounter with the Earth (and thus different values of  $\zeta$ ).

### 3.3. Shape and size of an impact keyhole

To compute the shape and size of an impact keyhole, we have to determine how the distance between two points of the  $b$ -plane of the current encounter varies, when considering their ‘images’ after propagation to the  $b$ -plane of the next encounter.

#### 3.3.1. The structure of the derivatives

Let us examine the structure of the derivatives of  $\xi''$ ,  $\zeta''$  as functions of  $\xi$ ,  $\zeta$  in the case in which  $c^2 \ll b^2$ , that is, for a dynamical evolution dominated by small deflection encounters. This assumption is not too severe: for the encounter of the asteroid 1997 XF<sub>11</sub> with the Earth in 2028,  $c \approx 1.4 \times 10^{-5}$ , and the local MOID is 0.000 19 AU, so that at most  $c/b \approx 0.076$ ,  $c^2/b^2 \approx 0.006$ ; for the encounter of 1999 AN<sub>10</sub> with the Earth in 2027,  $c \approx 3.9 \times 10^{-6}$ , and the local MOID is 0.000 25 AU, so that at most  $c/b \approx 0.016$ ,  $c^2/b^2 \approx 0.0003$ .

The partial derivatives have the form [12]

$$\begin{aligned} \frac{\partial \xi''}{\partial \xi} &= \frac{\partial \xi'}{\partial \xi}, \\ \frac{\partial \xi''}{\partial \zeta} &= \frac{\partial \xi'}{\partial \zeta}, \\ \frac{\partial \zeta''}{\partial \xi} &= \frac{\partial \zeta''}{\partial \theta'} \frac{\partial \theta'}{\partial \xi} + \frac{\partial \zeta'}{\partial \xi}, \\ \frac{\partial \zeta''}{\partial \zeta} &= \frac{\partial \zeta''}{\partial \theta'} \frac{\partial \theta'}{\partial \zeta} + \frac{\partial \zeta'}{\partial \zeta}. \end{aligned}$$

The matrix  $\partial(\xi', \zeta')/\partial(\xi, \zeta)$ , in turn, has the following structure

$$\begin{bmatrix} \frac{\partial \xi'}{\partial \xi} & \frac{\partial \xi'}{\partial \zeta} \\ \frac{\partial \zeta'}{\partial \xi} & \frac{\partial \zeta'}{\partial \zeta} \end{bmatrix} \approx \begin{bmatrix} 1 + \mathcal{O}(c/b) & \mathcal{O}(c/b) \\ \mathcal{O}(1) & 1 + \mathcal{O}(c/b) \end{bmatrix}.$$

That is, in the approximations used, the encounter is described by a nearly-area-preserving operator. The partial derivatives of  $\zeta''$  are

$$\begin{aligned} \frac{\partial \zeta''}{\partial \xi} &= h \cdot s(U', \theta') \cdot \frac{\partial \cos \theta'}{\partial \xi} + \frac{\partial \zeta'}{\partial \xi}, \\ \frac{\partial \zeta''}{\partial \zeta} &= h \cdot s(U', \theta') \cdot \frac{\partial \cos \theta'}{\partial \zeta} + \frac{\partial \zeta'}{\partial \zeta}. \end{aligned}$$

In each of them, the first term comes from the keplerian propagation, while the second comes from the first encounter.

The terms describing the keplerian propagation grow linearly with time due to the presence of  $h$ , and can become very large. In the majority of cases, that is, for a dynamical evolution dominated by small deflection encounters, and excluding tangential encounters ( $\sin \theta \neq 0$ ), the divergence of nearby trajectories is expressed by these terms. Note that the divergence of nearby orbits between consecutive encounters is linear in time, and that sequences of encounters result in the multiplicative accumulation of the divergence from each encounter, thus leading to exponential divergence and chaos, with maximum Lyapounov exponent proportional to encounter frequency.

Coming back to the shape and size of impact keyholes, we thus have that the ‘horizontal’ (i.e., along  $\xi$ ) distance on the  $b$ -plane is essentially unchanged, while the ‘vertical’ one (along  $\zeta$ ) is stretched by a large factor, that depends on the circumstances of the encounter.

The geometric consequence of this is that the ‘pre-image’ of the Earth on the  $b$ -plane of the encounter preceding the collision is a thick arclet closely following the shape of the circle corresponding to the suitable orbital period. The thickness of the arclet is inversely proportional to  $h \cdot s(U', \theta') \cdot \partial \cos \theta' / \partial \zeta$ .

#### 3.3.2. Application: the case of 1997 XF<sub>11</sub>

The pre-images of the Earth, corresponding to the two possible keyholes for a collision at a resonant return in 2040, are shown in Fig. 2. Both keyholes span, in  $\xi$ , roughly the diameter of the Earth augmented by the gravitational focusing; in  $\zeta$  a great compression is noticeable. The compression along  $\zeta$  is by a factor between 15 000 and 21 000 for the keyhole nearer to the Earth, and by a factor of about 124 for the other one, whose total area is thus much larger. Note that the compression factors

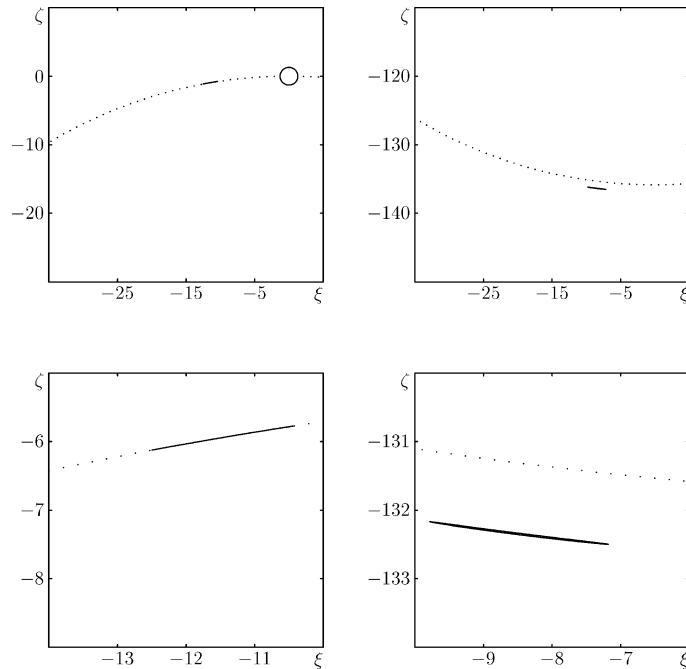


Fig. 2. Keyholes, in the  $b$ -plane of the October 2028 encounter with the Earth of 1997 XF<sub>11</sub>, for collision at the resonant return in 2040; units for the coordinates are Earth radii. Upper left: keyhole nearer to the Earth, with the latter shown to scale for comparison (the gravitational focusing is here about 30%); upper right: keyhole farther from the Earth; lower left and lower right: enlargements of, respectively, the near and far keyholes shown in the corresponding upper panels.

given here are different from those given in [12], where a similar computation was presented, in which a too high value for  $\xi$  was used.

A numerical integration, done with the software described in [2] and [7], shows that nearby trajectories actually diverge by a factor 131 between 2028 and 2040: thus, the result obtained analytically by using the extended Öpik is well within 10% of the numerical one, a quite satisfactory achievement, given the approximations involved.

#### 4. Conclusions

In the long term, asteroid impacts represent a potential major threat to mankind. Currently, two independent orbit computation centres routinely check the confidence regions, about the orbits of all NEAs, for Earth impact possibilities in the next decades [7,8]. This has been made possible by the ability to set up numerical algorithms able to disentangle and analyze the cascade of returns to Earth encounter after the occurrence of a first close approach.

I have summarized the current status of the geometrical understanding of the problem of resonant returns, using as a guide the analytical theory that has been developed in recent years along the lines first introduced by Öpik.

#### Acknowledgements

Many people contributed over the last twenty years to the development of the theory presented here. I am grateful to all of them and in particular, for the most recent advancements, to A. Milani, S.R. Chesley and G.F. Gronchi. I am especially indebted to A. Rossi for his comments on the manuscript.

#### References

- [1] A.J. Lexell, Reflexions sur le temps périodique des Comètes en général & principalement sur celui de la Comète observée en 1770, Acta Acad. Sci. Imper. Petropol., pars posterior (1778), 12–34, published in 1781.

- [2] A. Milani, S.R. Chesley, G.B. Valsecchi, Close approaches of asteroid 1999 AN<sub>10</sub>: resonant and non-resonant returns, *Astron. Astrophys.* 346 (1999) L65–L68.
- [3] U.-J. Le Verrier, Théorie de la comète périodique de 1770, *C. R. Acad. Sci. Paris* 19 (1844) 982–994.
- [4] U.-J. Le Verrier, Mémoire sur de la comète périodique de 1770, *C. R. Acad. Sci. Paris* 26 (1848) 465–469.
- [5] U.-J. Le Verrier, Théorie de la comète périodique de 1770, *Ann. Obs. Paris* 3 (1857) 203–270.
- [6] A. Carusi, M. Kresáková, G.B. Valsecchi, Perturbations by Jupiter of the particles ejected from Comet Lexell, *Astron. Astrophys.* 116 (1982) 201–209.
- [7] A. Milani, S.R. Chesley, G.B. Valsecchi, Asteroid close encounters with the Earth: risk assessment, *Planet. Space Sci.* 48 (2000) 945–954.
- [8] A.B. Chamberlin, S.R. Chesley, P.W. Chodas, J.D. Giorgini, M.S. Keesey, R.N. Wimberly, D.K. Yeomans, Sentry: an automated close approach monitoring system for near-earth objects, *Bull. Amer. Astron. Soc.* 33 (2001) 1116.
- [9] A. Milani, S.R. Chesley, M.E. Sansaturio, G. Tommei, G.B. Valsecchi, Nonlinear impact monitoring: line of variation searches for impactors, *Icarus* (2005), in press.
- [10] E.J. Öpik, *Interplanetary Encounters*, Elsevier, New York, 1976.
- [11] A. Carusi, G.B. Valsecchi, R. Greenberg, Planetary close encounters: geometry of approach and post-encounter orbital parameters, *Celest. Mech. Dynam. Astron.* 49 (1990) 111–131.
- [12] G.B. Valsecchi, A. Milani, G.F. Gronchi, S.R. Chesley, Resonant returns to close approaches: analytical theory, *Astron. Astrophys.* 408 (2003) 1179–1196.
- [13] G.F. Gronchi, A. Milani, Proper elements for earth-crossing asteroids, *Icarus* 152 (2001) 58–69.
- [14] P.W. Chodas, *Bull. Amer. Astron. Soc.* 31 (1999) 1117.
- [15] G.B. Valsecchi, A. Milani, G.F. Gronchi, S.R. Chesley, The distribution of energy perturbations at planetary close encounters, *Celest. Mech. Dynam. Astron.* 78 (2000) 83–91.
- [16] A. Milani, The asteroid identification problem, *Icarus* 137 (1999) 269–292.